Electronic supplementary information

Synthesis and hierarchical self-assembly of luminescence platinum(II)-containing telechelic metallopolymers

Xiandeng Qiu,[†] Hua Xue,[†] Lin Xu,[†] Ran Wang,[†] Shengchao Qiu,[†] Qun He[†] and Weifeng Bu[*,†,‡]

[†]State Key Laboratory of Applied Organic Chemistry, Key Laboratory of Nonferrous Metals Chemistry and Resources Utilization of Gansu Province, and College of Chemistry and Chemical Engineering, Lanzhou University, Lanzhou, 730000, China

[‡]State Key Laboratory of Solid Lubrication, Lanzhou Institute of Chemical Physics, Chinese Academy of Sciences, Lanzhou, 730000, China

Corresponding Author

*E-mail: buwf@lzu.edu.cn

Experimental Section

General Considerations. Styrene and cuprous bromide (CuBr) were purchased from *Sinopharm Chemical*. Before use, they were respectively purified under reduced pressure and *via* washing with glacial acetic acid. Other commercially available solvents and chemicals were directly used without any further purification. Iodomethane, 1,12-dibromododecane, diethyl 2,5-dibromoadipate, *N*,*N*,*N*′,*N*″,*N*″-pentamethyldiethylenetriamine (PMDETA), tetrabutylammonium iodide (TBAI) were obtained from *Energy Chemical*. 2-(Methylbenzimidazol-2′-yl)-6-(benzimidazol-2′-yl)pyridine (Mebzimpy),[S1] 4-(12-bromododecyloxy)phenylacetylene (Br-PA),[S2] and 4-[(4′-ethynylphenyl)oxy]dodecyloxy-2,6-bis(*N*-methylbenzimidazol-2′-yl)pyridine (**L-II**)[S3] were synthesized as described in the previous literatures.

^{1}H and ^{13}C NMR spectra were recorded on a *JNM-ESC400* spectrometer, during which the samples were dissolved in *d*-chloroform ($CDCl_3$) and tetramethylsilane was used as an internal standard. High-resolution electrospray ionization mass spectra (HR-ESI-MS) were obtained on a *Bruker APEX II FT-MS* mass spectrometer. Matrix-assisted laser desorption/ionization time-of-flight (MALDI-TOF) mass spectra were acquired on a *SHIMADZU MALDI-7090* mass spectrometer. Gel permeation chromatography (GPC) plots were recorded on a *Waters 1515 instrument* and determined the values of number-average molecular weight (M_n), weight-average molecular weight (M_w), and polydispersity index (PDI) of telechelic polystyrenes (**TPS$_{2n}$L-I** and **TPS$_{2n}$L-II**). Polystyrene was used as a calibration standard, and tetrahydrofuran (THF) was the eluent at a flow rate of 1.0 mL/min. The column temperature was kept at 40 °C. UV-vis absorption spectra were recorded by using a *SHIMADZU UV-2550* spectrophotometer. Luminescence measurements were made on a Hitachi-7000 spectrofluorometer with a xenon lamp as the excitation source (150 W). The corresponding emission and excitation wavelengths were set at 615 and 420 nm, respectively. Luminescence quantum yields (Φ) were estimated by using $[Ru(bpy)_3]Cl_2$ in water (Φ = 0.040 in air) as a standard.[S4,S5] Luminescence lifetimes were measured on an Edinburgh Instruments FSL920 fluorescence spectrometer, during which a supercontinuum laser was used as the excitation source. Dynamic light scattering (DLS) measurements were performed on a *Brookhaven BI-200SM* spectrometer. Transmission electron microscopy (TEM) images were performed with an FEI Tecnai F30 operating at 300 kV or a JEM-2100 operating at 200 kV. Scanning electron microscopy (SEM) measurements were performed on a *field emission Hitachi S-4800*. Before the imaging, thin gold layers (ca. 5 nm) were coated on the specimen by using a Hitachi E-1045 ion sputter. All measurements were performed at 20 °C except for GPC under the temperature of 40 °C.

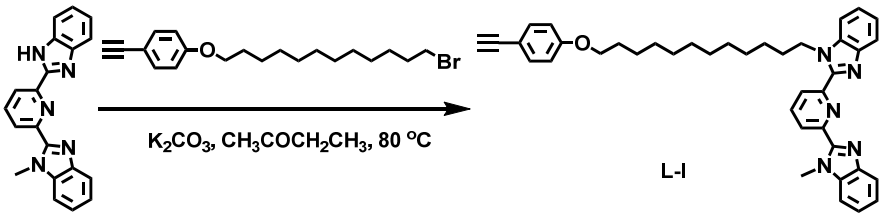

Fig. S1 The synthetic procedure of **L-I**.

Synthetic Procedures and Characterization Details.

L-I: Mebzimpy[S1] (1 g, 2.08 mmol), Br-PA[S2] (914 mg, 2.5 mmol), K_2CO_3 (719 mg, 5.2 mmol),

KI (346 mg, 2.08 mmol), and 18-crown-6 (5.6 mg, 0.021 mmol) were added to 2-butanone (50 mL) in an oven dried Schlenk flask under an argon atmosphere. The resulting mixture was stirred at 80 °C for 4 days. After cooling to room temperature, the insoluble solid was removed by filtration and then the solvent was removed under reduced pressure. Further purification by column chromatography on silica gel using petroleum ether–dichloromethane (v/v = 2/1) yielded a yellow oily product (1.17 g, 93% yield).

^{1}H NMR (400 MHz, $CDCl_3$, ppm), δ: 0.98-1.28 (m, 14H, CH_2), 1.39 (m, 2H, CH_2), 1.74 (m, 4H, CH_2), 2.99 (s, 1H), 3.93 (t, J = 8.0 Hz, 2H, $ArOCH_2$), 4.19 (s, 3H, NCH_3), 4.77 (t, J = 8.0 Hz, 2H, NCH_2), 6.81 (d, J = 8.0 Hz, 2H, Ar), 7.30-7.43 (m, 6H, Ar), 7.44-7.50 (m, 2H, Ar), 7.89 (d, J = 8.0 Hz, 2H, Ar), 8.05 (t, J = 8 Hz, 1H), 8.37 (d, J = 8 Hz, 2H). ^{13}C NMR (100 MHz, $CDCl_3$, ppm), δ: 26.05, 26.76, 29.15, 29.12, 29.15, 29.21, 29.38, 29.43, 29.48, 30.15, 32.46, 44.96, 53.54, 68.11, 75.75, 83.85, 110.03, 110.47, 113.91, 114.51, 120.34, 120.40, 122.84, 122.99, 123.60, 123.73, 125.53, 133.65, 136.45, 137.21, 138.22, 142.73, 142.86, 149.72, 150.09, 150.52, 159.61. HR-ESI-MS: *m/z* calcd for $[M+H]^+$: 610.3540. Found: 610.3546.

$TPS_{78}Br$: Under an atmosphere of Ar, CuBr (0.115 g, 0.800 mmol), diethyl 2,5-dibromoadipate (0.120 g, 0.333 mmol), and PMDETA (0.181 mL, 0.930 mmol) were dissolved in styrene (20 g, 192 mmol) in a round-bottom flask. The feeding molar ratio between styrene and diethyl 2,5-dibromoadipate was controlled at 570:1. The resulting mixture was degassed by three freeze–pump–thaw cycles, sealed under vacuum, and further placed in an oil bath preheated at 90 °C for 45 min, during which the solution gradually became viscous. After cooling the reaction mixture to room temperature, CH_2Cl_2 (5 mL) was added under ambient condition. Then the CH_2Cl_2 solution was passed through a neutral alumina column to remove the copper catalyst. The filtrate was concentrated to ca. 8 mL and then precipitated into 200 mL of methanol for three times. The solids were subsequently collected *via* vacuum filtration, and then dried under vacuum to afford 2.2 g as a white powder. GPC: M_n = 8200, PDI = 1.08.

$TPS_{2n}Br$ ($2n$ = 26, 40, 60, 98, 118, 158) were synthesized by following the procedure depicted for **$TPS_{78}Br$**. The feeding molar ratios between styrene and diethyl 2,5-dibromoadipate was controlled at 230:1, 290:1, 380:1, 690:1, 820:1 and 920:1, respectively. The M_n and PDI values were determined by GPC measurements and further recorded in Table S1.

$TPS_{78}N_3$: $TPS_{78}Br$ (2 g, 0.247 mmol), NaN_3 (160 mg, 2.47 mmol), TBAI (18 mg, 0.049 mmol) were added to DMF (20 mL) in an oven dried Schlenk flask under an argon atmosphere. The resulting mixture was stirred at 55 °C for 3 days. The reaction mixture was cooled to room temperature and the solvent was removed under reduced pressure. After removing the solvent, the crude product was dissolved in 5 mL of CH_2Cl_2 and then precipitated into 150 mL of methanol for three times. The solids were subsequently collected *via* vacuum filtration and then dried under vacuum to afford 1.9 g (95% yield) as a white powder. GPC: M_n = 8800, PDI = 1.08.

$TPS_{2n}N_3$ (n = 26, 40, 60, 98, 118, 158) were synthesized by following the procedure depicted for **$TPS_{78}N_3$**, but by using **$TPS_{2n}Br$** ($2n$ = 26, 40, 60, 98, 118, 158) as the reaction precursors, respectively.

TPS_{78}L-I: To a mixture solution of **$TPS_{78}N_3$** (1.5 g, 0.370 mmol $-N_3$ group) and **L-I** (384 mg, 0.632 mmol) in THF/DMF (5 mL/5 mL) in a Schlenk flask, CuBr (72 mg, 0.500 mmol) and PMDETA (108 μL, 0.556 mmol) were added successively under an argon atmosphere. This reaction system was further deoxygenated by three freeze–pump–thaw cycles. The resulting solution was placed in a thermostatic oil bath held at 80 °C and stirred for 3 days. The crude product was diluted

with CH_2Cl_2 and passed through a column of neutral alumina to remove the copper catalyst. The sample was further purified by precipitating its concentrated CH_2Cl_2 solution in cold methanol three times and dried in a vacuum oven at 45 °C. And then, a white solid was obtained with a yield of 96% (1.64 g) on the basis of **TPS$_{78}$N$_3$**. GPC: M_n = 9400, PDI = 1.07.

TPS$_{2n}$L-I (2n = 26, 40, 60, 98, 118, 158) were synthesized by following the procedure depicted for **TPS$_{78}$L-I**, but by using **TPS$_{2n}$N$_3$** (2n = 26, 40, 60, 98, 118, 158) as the reaction precursors, respectively. The polymer ligands of **TPS$_{2n}$L-II** were similarly prepared by reacting the **TPS$_{2n}$N$_3$** precursors with **L-II**[S3]. The isolated yields for these polymeric ligands were equal to or larger than 95% on the basis of **TPS$_{2n}$N$_3$**.

TPS$_{78}$Pt-I: TPS$_{78}$L-I (1 g, 0.212 mmol **L-I** group), K_2PtCl_4 (104 mg, 0.254 mmol) were added to DMSO/$CHCl_3$ (10 mL/30 mL) in an oven dried Schlenk flask under an argon atmosphere. The resulting mixture solution was placed in a thermostatic oil bath held at 90 °C and stirred for 4 days. The orange solution was cooled to room temperature and the solvents were removed by distilling under vacuum conditions. A red solid was collected by filtration and further washed with cold methanol (100 mL). The yield was 92% (0.97 g) based on the **TPS$_{78}$L-I** ligand.

According to the synthetic procedure of **TPS$_{78}$Pt-I**, **TPS$_{2n}$Pt-I** (2n = 26, 40, 60, 98, 118, 158) were prepared similarly, but by using **TPS$_{2n}$L-I** (2n = 26, 40, 60, 98, 118, 158) as the reaction precursors, respectively. The metallopolymers of **TPS$_{2n}$Pt-II** (2n = 26, 40, 60, 78, 98, 118, 158) were similarly synthesized by reacting **TPS$_{2n}$L-II** with K_2PtCl_4. All of the isolated yields were equal to or larger than 90% on the basis of the corresponding ligands (Table 1).

Table S1 Molecular characteristics of **TPS$_{2n}$Br** (n = 13, 20, 30, 49, 59, 79)

Sample	M_n [a] / g mol^{-1}	M_w/M_n [a]	Sample	M_n [a] / g mol^{-1}	M_w/M_n [a]
TPS$_{26}$Br	2600	1.11	**TPS$_{98}$Br**	10200	1.07
TPS$_{40}$Br	4200	1.08	**TPS$_{118}$Br**	12200	1.07
TPS$_{60}$Br	6200	1.09	**TPS$_{158}$Br**	16400	1.08
TPS$_{78}$Br	8200	1.08			

[a] The values of M_n, M_w, and M_w/M_n (PDI) were determined by GPC.

Table S2 The luminescence lifetimes and quantum yields of **TPS_{78}Pt-I** and **TPS_{118}Pt-II** dispersed in the chloroform/methanol mixture solvents.

sample	methanol volume ratio	Φ / % [a]	τ_1 / ns [b]	τ_2 / ns [b]	τ_3 / ns [b]
TPS_{78}Pt-I	0	0.68	5.88	32.7	78.2
TPS_{78}Pt-I	50%	7.70	50.0	280	-
TPS_{78}Pt-I	67%	9.74	108	388	-
TPS_{78}Pt-I	75%	5.22	89.1	380	-
TPS_{78}Pt-I	90%	6.19	100	412	-
TPS_{118}Pt-II	0	1.25	9.48	33.1	125
TPS_{118}Pt-II	50%	4.76	26.2	112	246
TPS_{118}Pt-II	67%	6.59	60.7	226	-
TPS_{118}Pt-II	75%	7.82	59.1	226	-
TPS_{118}Pt-II	90 %	7.32	81.4	307	-

[a] $[Ru(bpy)_3]Cl_2$ was used as a reference in water (Φ = 0.040 in air). [b] Relative weighting (RW) of components in double- or triple- exponential fits.

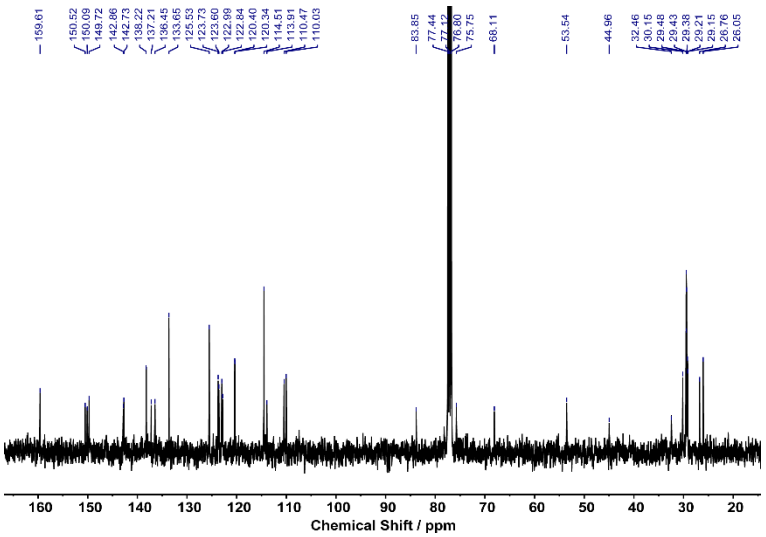

Fig. S2 ^{13}C NMR spectrum of **L-I**.

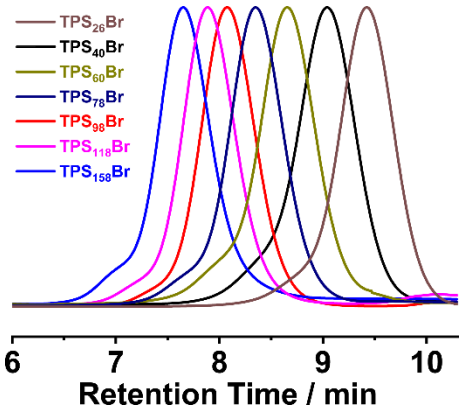

Fig. S3 GPC traces of **TPS$_{2n}$Br** ($2n$ = 26, 40, 60, 78, 98, 118, 158).

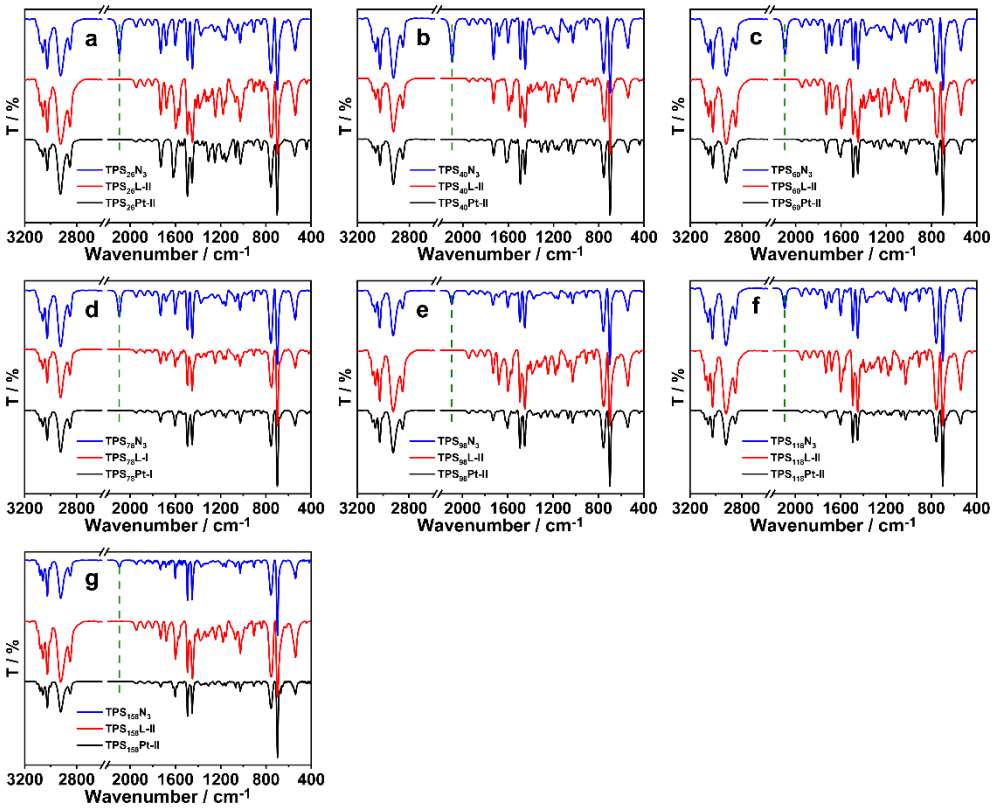

Fig. S4 FT-IR spectra of **TPS$_{2n}$N$_3$**, **TPS$_{2n}$L-I**, and **TPS$_{2n}$Pt-I** (2*n* = 26, 40, 60, 78, 98, 118, 158).

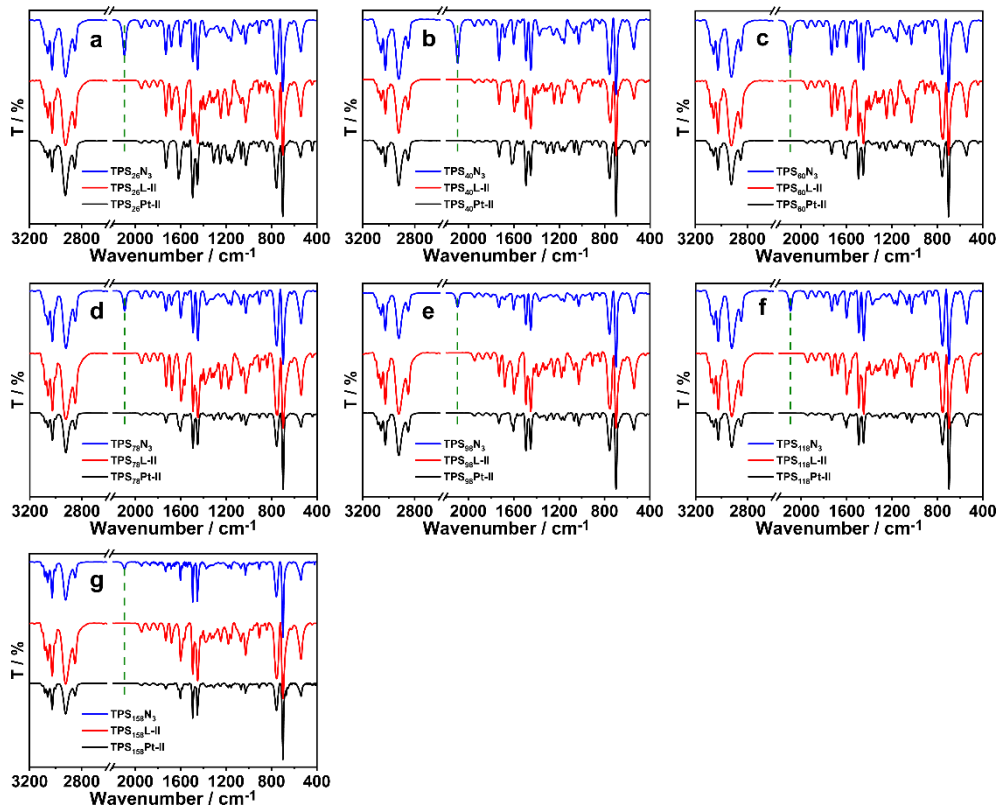

Fig. S5 FT-IR spectra of **TPS$_{2n}$N$_3$**, **TPS$_{2n}$L-II**, and **TPS$_{2n}$Pt-II** (2*n* = 26, 40, 60, 78, 98, 118, 158).

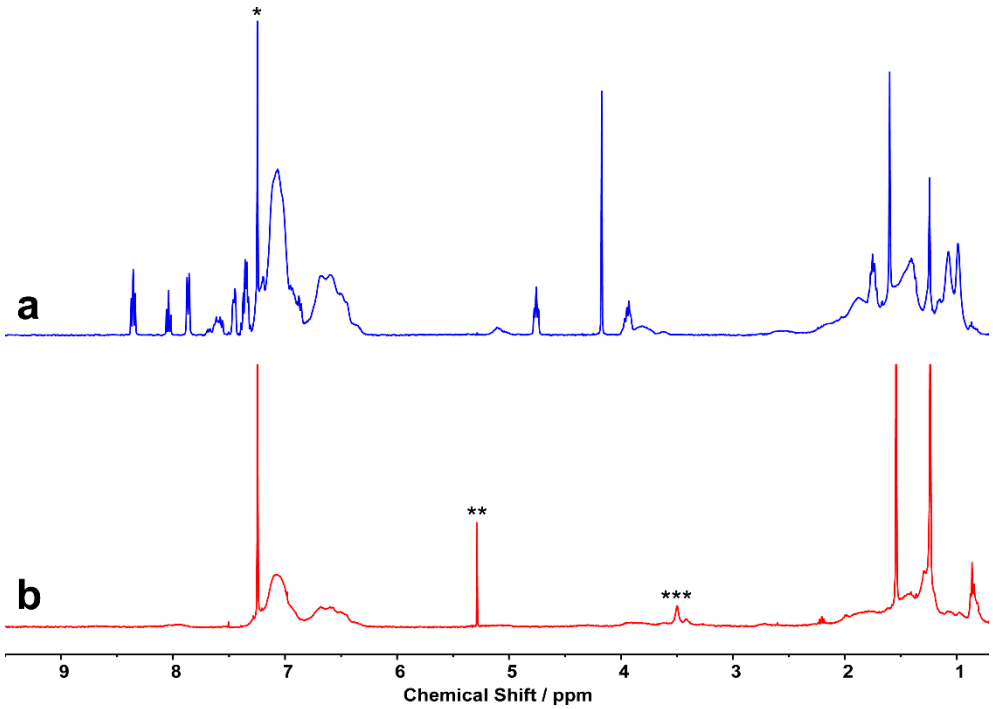

Fig. S6 ^{1}H NMR spectra of **TPS$_{26}$L-I** (a) and **TPS$_{26}$Pt-I** (b). The ∗, ∗∗, and ∗∗∗ signals referred to the residual solvents of $CHCl_3$, CH_2Cl_2, and CH_3OH, respectively.

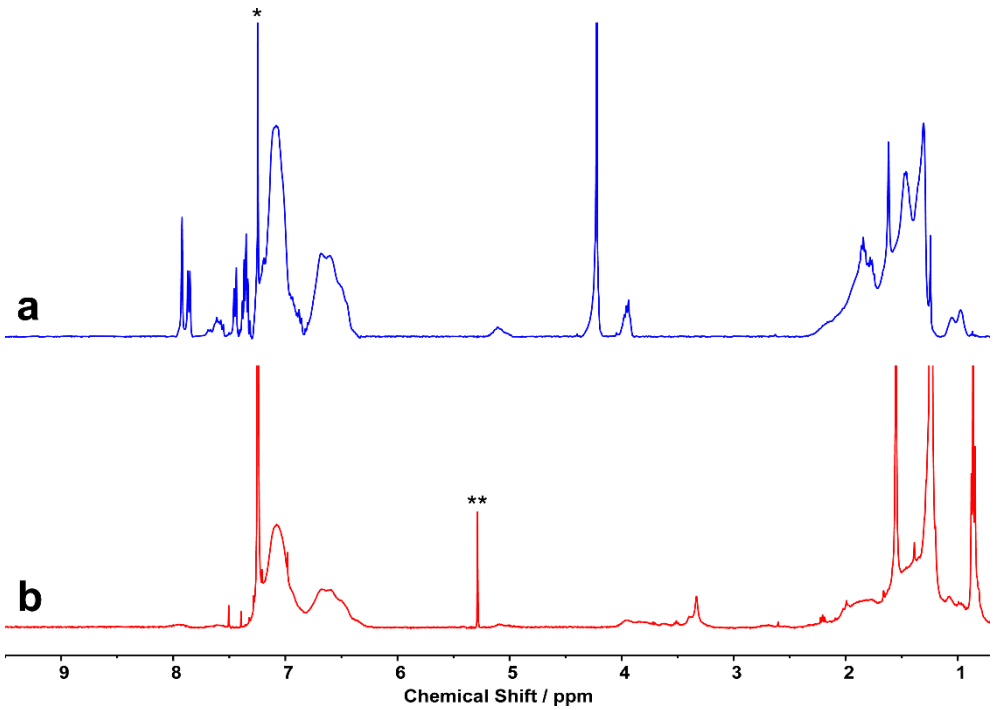

Fig. S7 ^{1}H NMR spectra of **TPS$_{26}$L-II** (a) and **TPS$_{26}$Pt-II** (b). The ∗ and ∗∗ signals referred to the residual solvents of $CHCl_3$ and CH_2Cl_2, respectively.

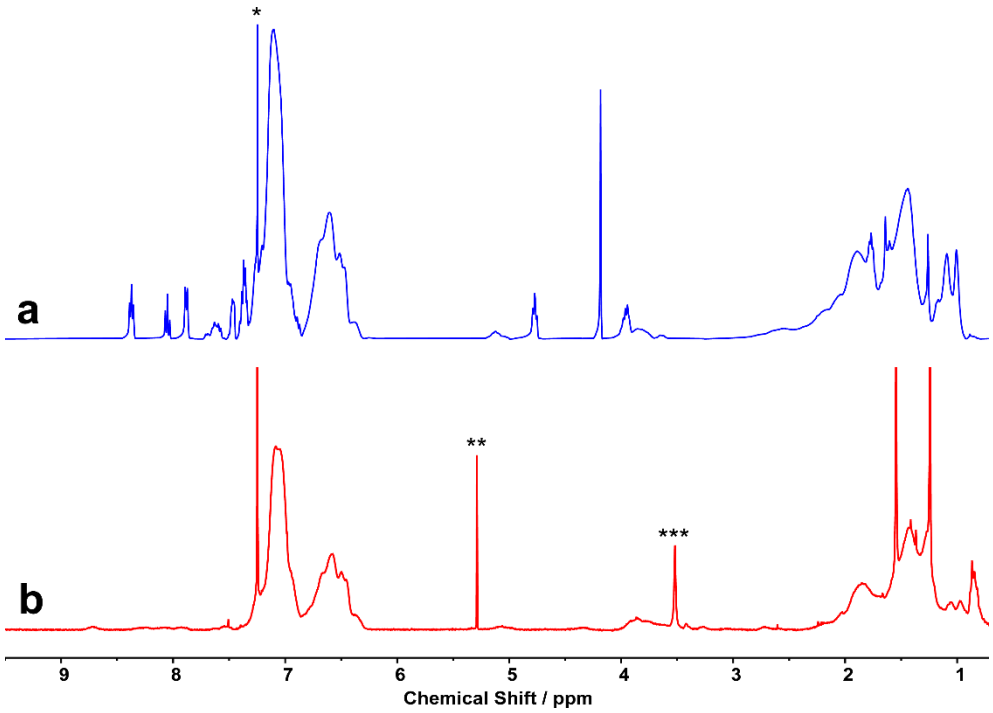

Fig. S8 ^{1}H NMR spectra of **TPS$_{40}$L-I** (a) and **TPS$_{40}$Pt-I** (b). The ∗, ∗∗, and ∗∗∗ signals referred to the residual solvents of $CHCl_3$, CH_2Cl_2, and CH_3OH, respectively.

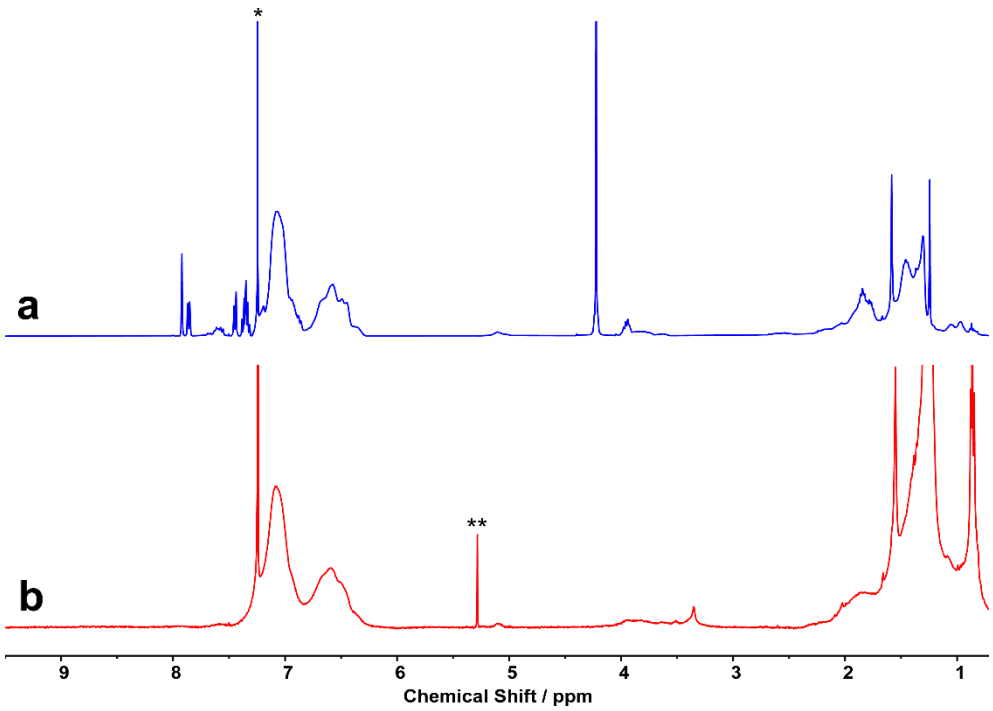

Fig. S9 ^{1}H NMR spectra of **TPS$_{40}$L-II** (a) and **TPS$_{40}$Pt-II** (b). The ∗ and ∗∗ signals referred to the residual solvents of $CHCl_3$ and CH_2Cl_2, respectively.

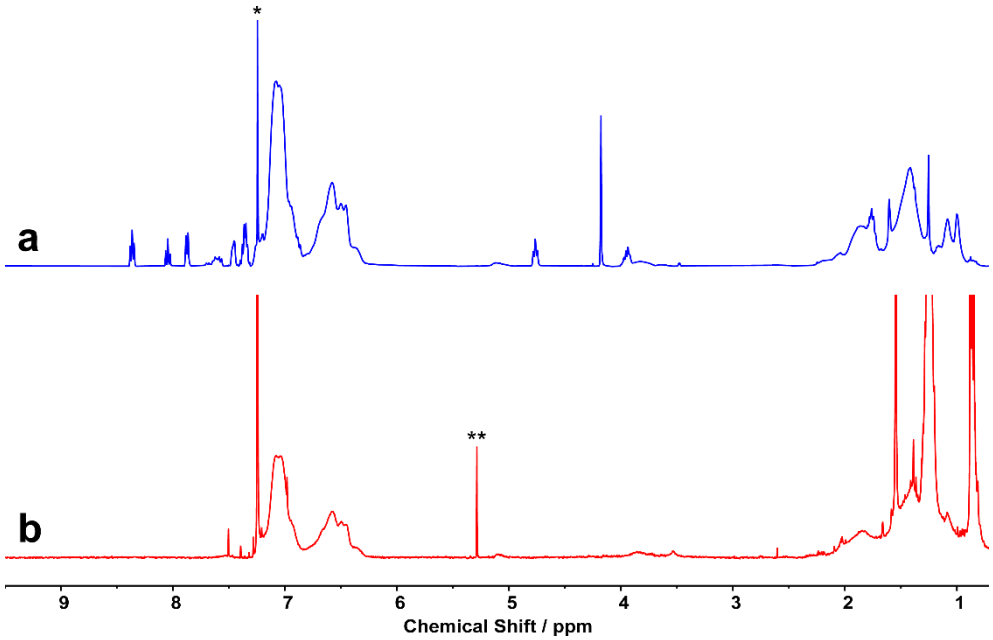

Fig. S10 ^{1}H NMR spectra of **TPS$_{60}$L-I** (a) and **TPS$_{60}$Pt-I** (b). The ∗ and ∗∗ signals referred to the residual solvents of $CHCl_3$ and CH_2Cl_2, respectively.

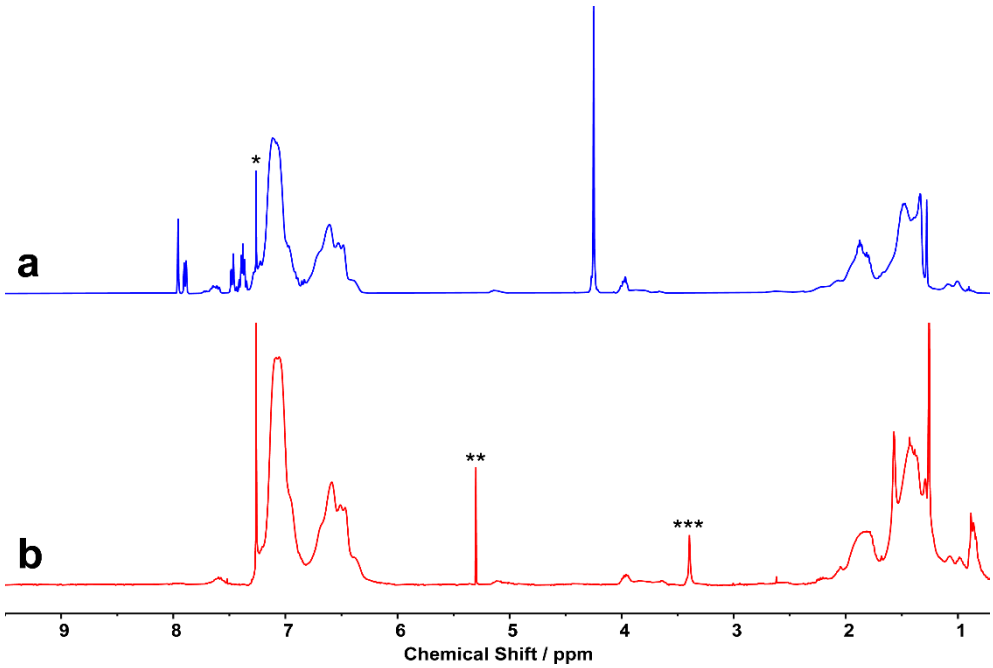

Fig. S11 ^{1}H NMR spectra of **TPS$_{60}$L-II** (a) and **TPS$_{60}$Pt-II** (b). The ∗, ∗∗, and ∗∗∗ signals referred to the residual solvents of $CHCl_3$, CH_2Cl_2, and CH_3OH, respectively.

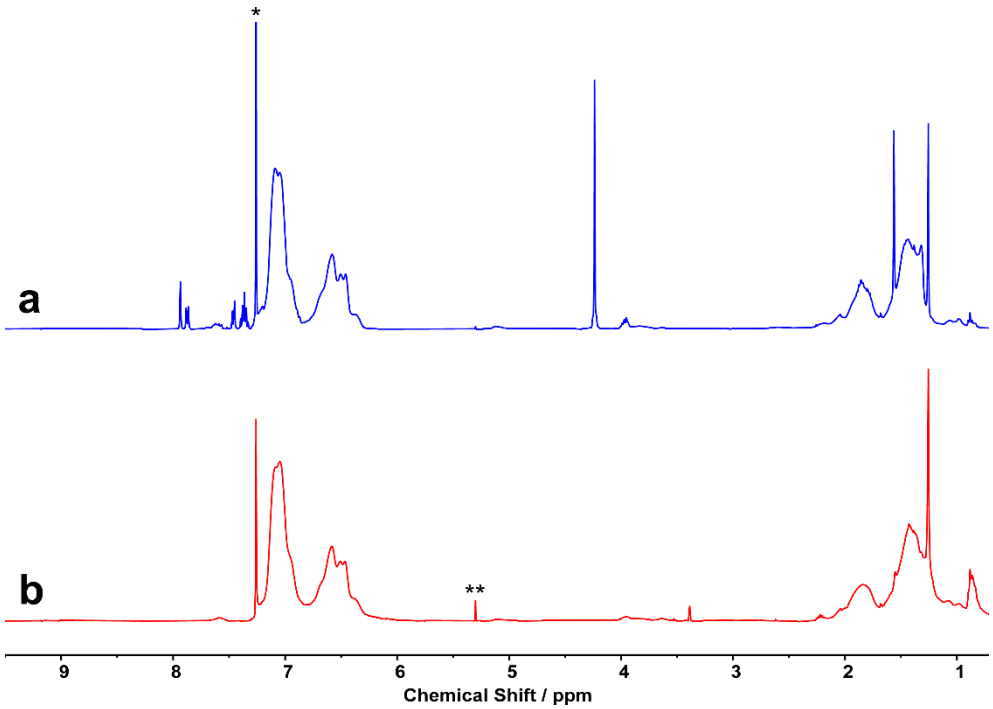

Fig. S12 ^{1}H NMR spectra of **TPS$_{78}$L-II** (a) and **TPS$_{78}$Pt-II** (b). The ∗ and ∗∗ signals referred to the residual solvents of $CHCl_3$ and CH_2Cl_2, respectively.

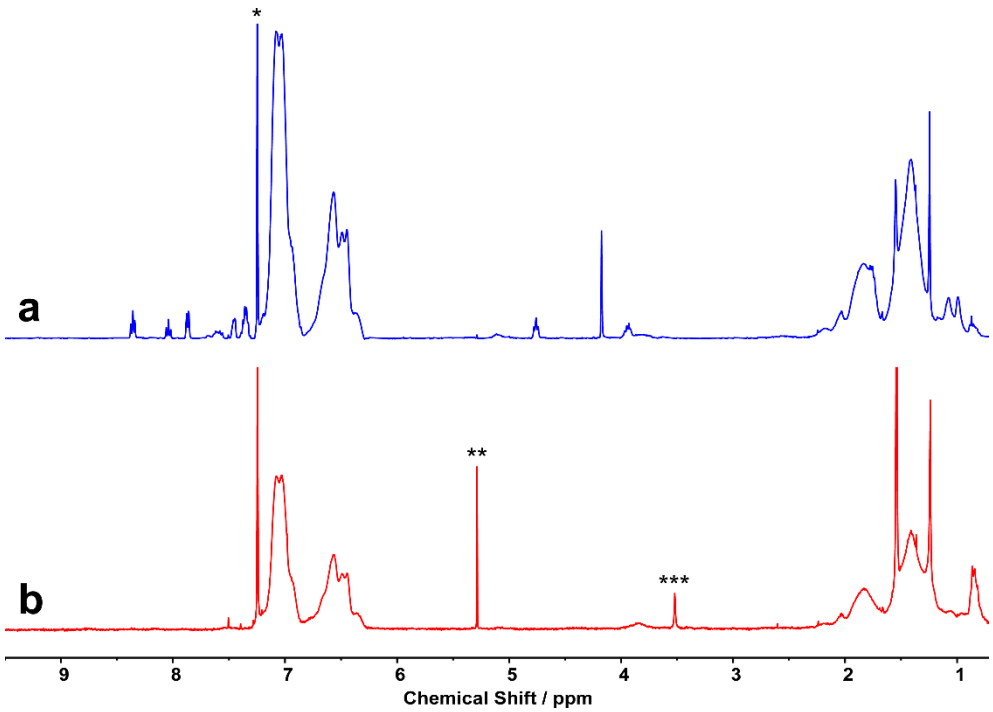

Fig. S13 ^{1}H NMR spectra of **TPS$_{98}$L-I** (a) and **TPS$_{98}$Pt-I** (b). The ∗, ∗∗, and ∗∗∗ signals referred to the residual solvents of $CHCl_3$, CH_2Cl_2, and CH_3OH, respectively.

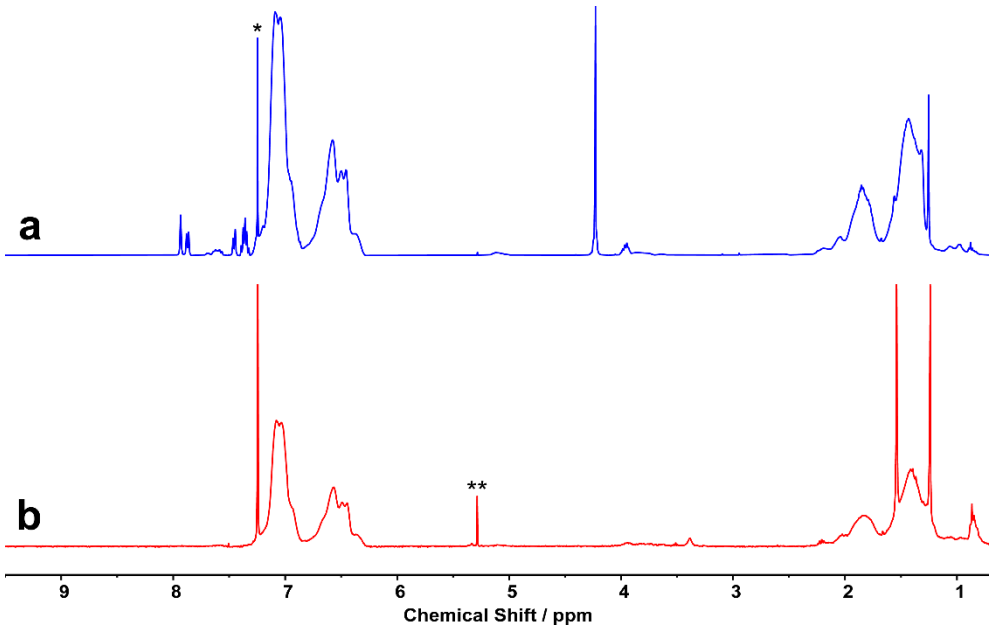

Fig. S14 ^{1}H NMR spectra of **TPS$_{98}$L-II** (a) and **TPS$_{98}$Pt-II** (b). The ∗ and ∗∗ signals referred to the residual solvents of $CHCl_3$ and CH_2Cl_2, respectively.

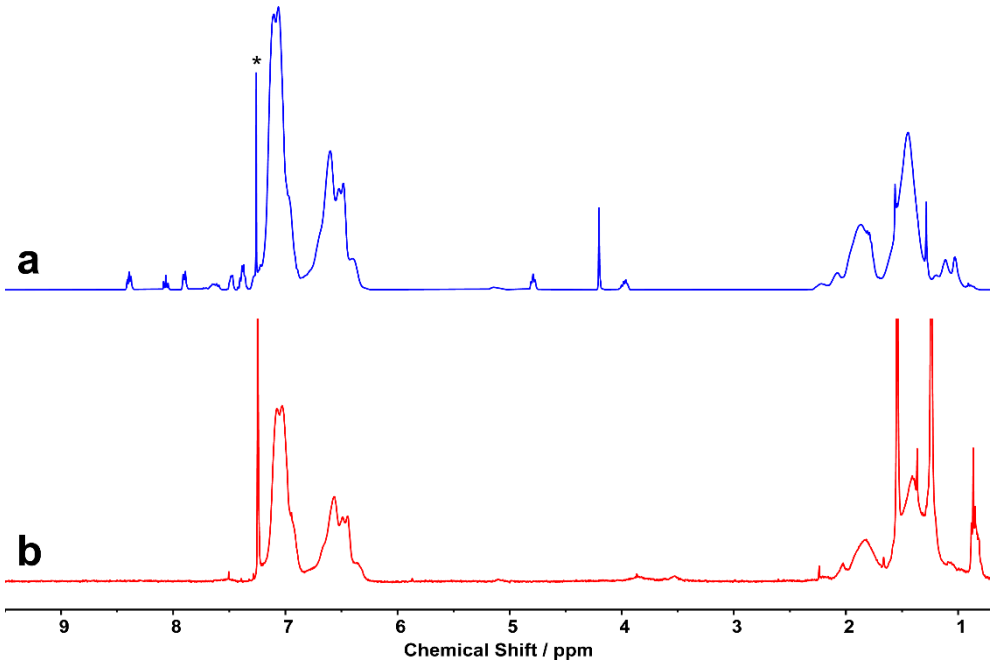

Fig. S15 ^{1}H NMR spectra of **TPS$_{118}$L-I** (a) and **TPS$_{118}$Pt-I** (b). The ∗ signals referred to the residual solvents of $CHCl_3$.

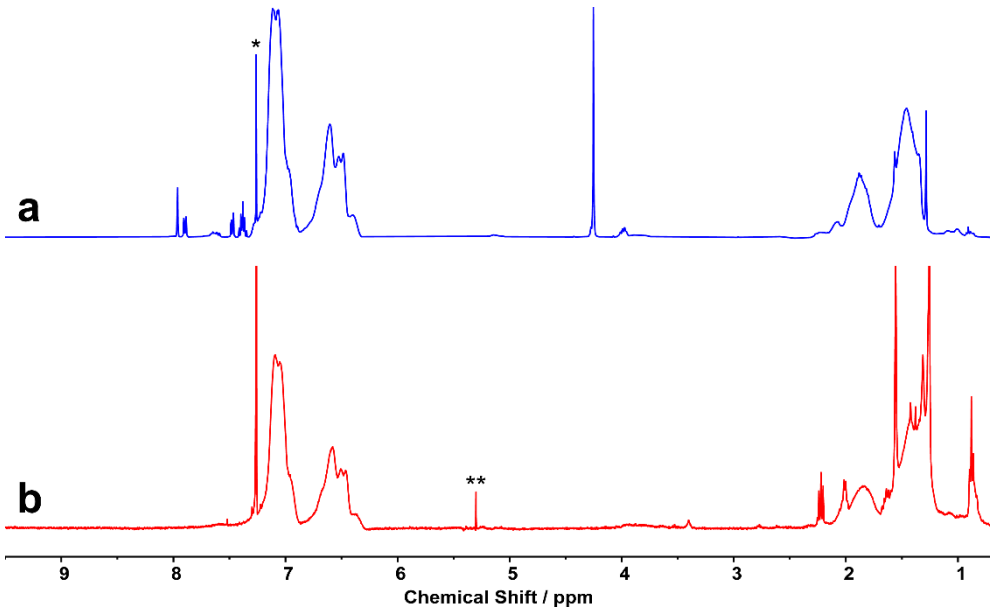

Fig. S16 ^{1}H NMR spectra of **TPS$_{118}$L-II** (a) and **TPS$_{118}$Pt-II** (b). The ∗ and ∗∗ signals referred to the residual solvents of $CHCl_3$ and CH_2Cl_2, respectively.

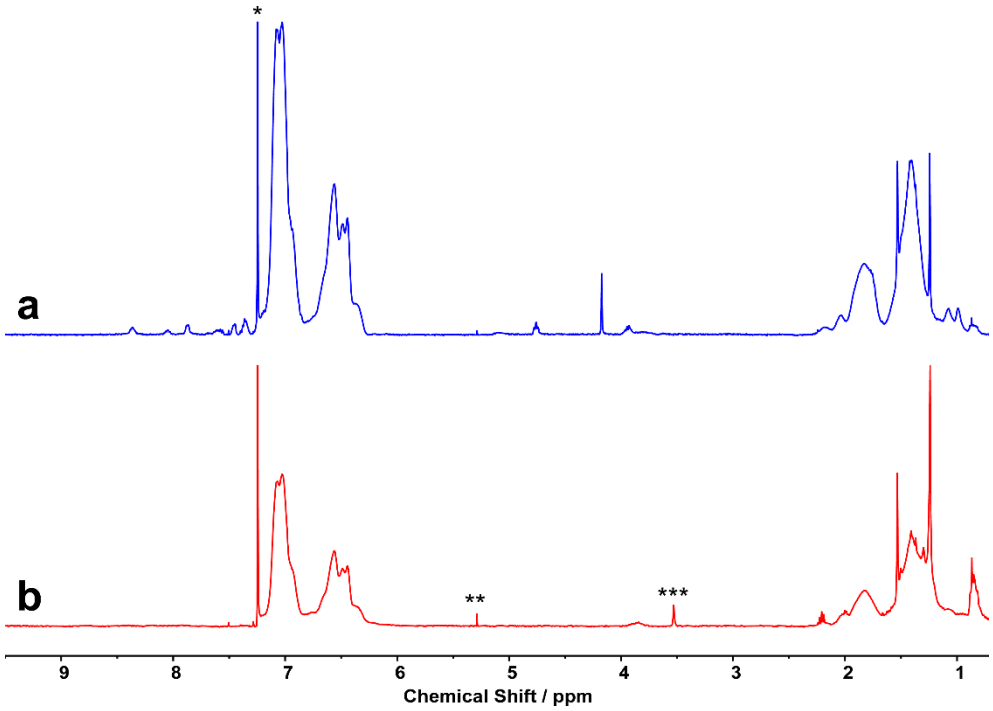

Fig. S17 ^{1}H NMR spectra of **TPS$_{158}$L-I** (a) and **TPS$_{158}$Pt-I** (b). The ∗, ∗∗, and ∗∗∗ signals referred to the residual solvents of $CHCl_3$, CH_2Cl_2, and CH_3OH, respectively.

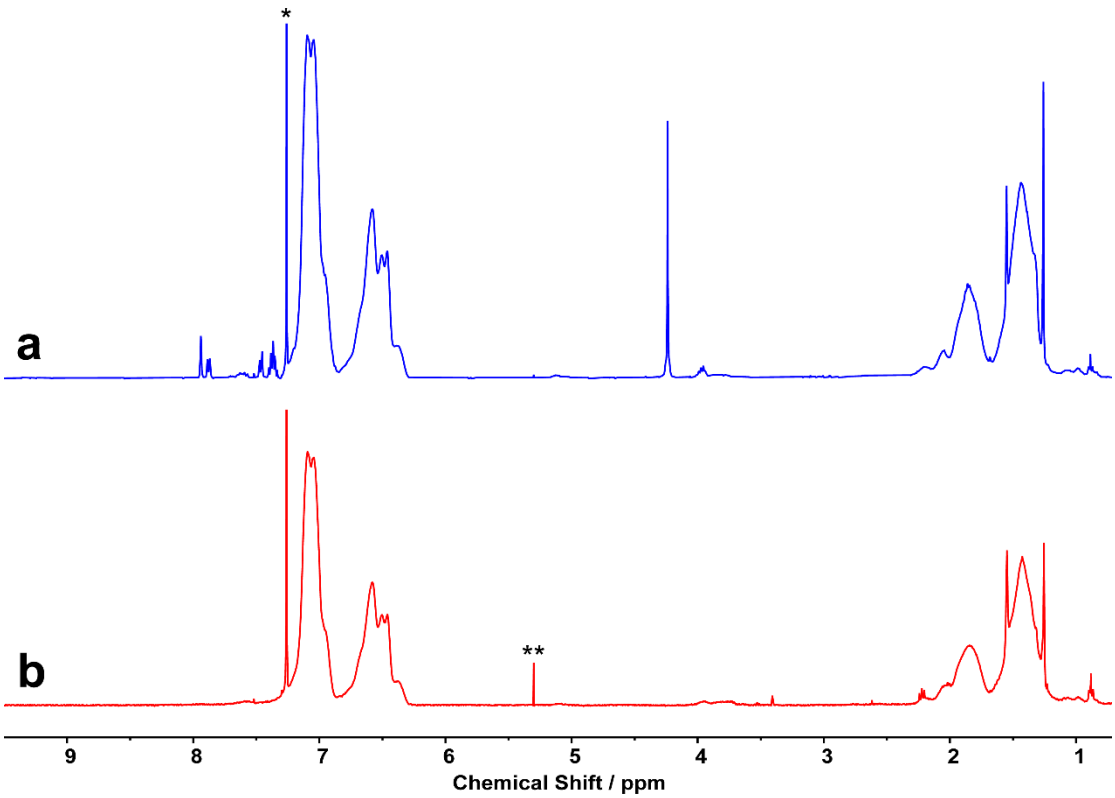

Fig. S18 ^{1}H NMR spectra of **TPS$_{158}$L-II** (a) and **TPS$_{158}$Pt-II** (b). The ∗ and ∗∗ signals referred to the residual solvents of $CHCl_3$ and CH_2Cl_2, respectively.

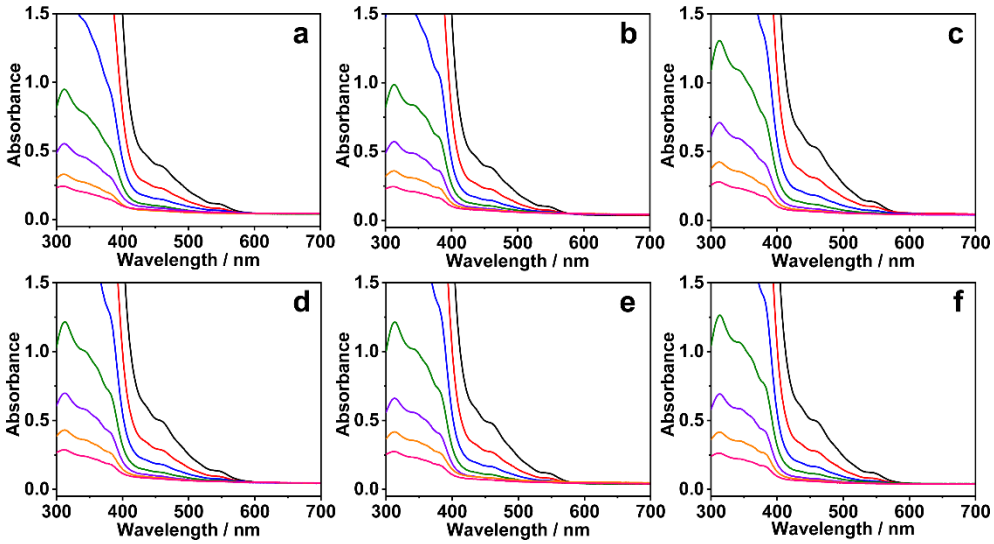

Fig. S19 UV-vis absorption of **TPS$_{26}$Pt-I** (a), **TPS$_{40}$Pt-I** (b), **TPS$_{60}$Pt-I** (c), **TPS$_{98}$Pt-I** (d), **TPS$_{118}$Pt-I** (e), and **TPS$_{158}$Pt-I** (f) in chloroform with the increasing concentration (3.12×10^{-6}, 6.25×10^{-6}, 1.25×10^{-5}, 2.5×10^{-5}, 5.0×10^{-5}, 1.0×10^{-4}, and 2×10^{-4} mol/L).

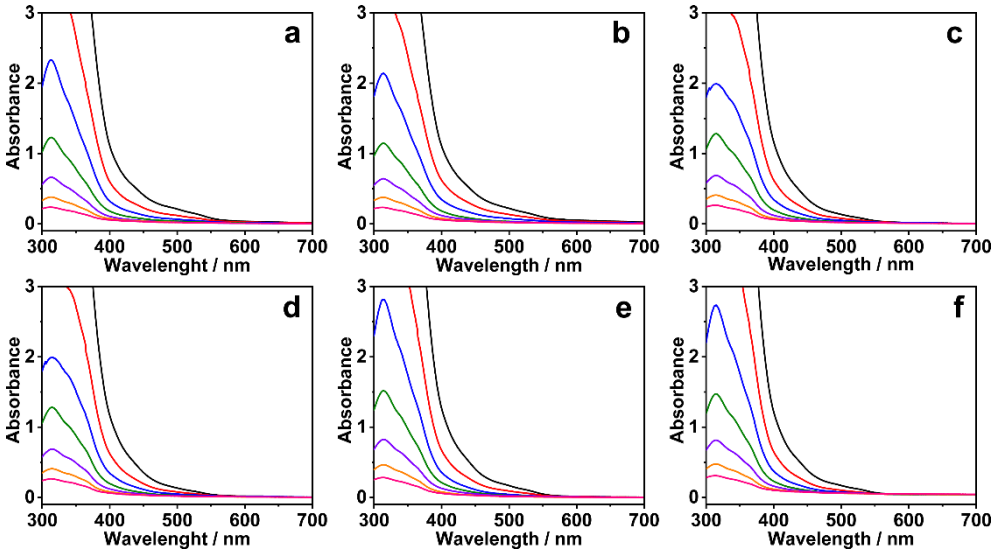

Fig. S20 UV-vis absorption of **TPS$_{26}$Pt-II** (a), **TPS$_{40}$Pt-II** (b), **TPS$_{60}$Pt-II** (c), **TPS$_{78}$Pt-II** (d), **TPS$_{98}$Pt-II** (e), and **TPS$_{158}$Pt-II** (f) in chloroform with the increasing concentration (3.12×10^{-6}, 6.25×10^{-6}, 1.25×10^{-5}, 2.5×10^{-5}, 5.0×10^{-5}, 1.0×10^{-4}, and 2×10^{-4} mol/L).

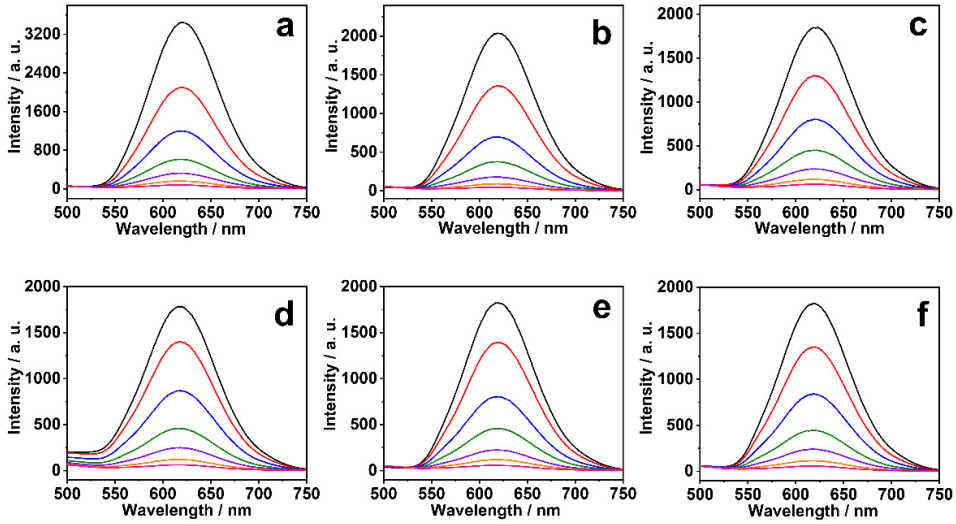

Fig. S21 Luminescence spectra of **TPS$_{26}$Pt-I** (a), **TPS$_{40}$Pt-I** (b), **TPS$_{60}$Pt-I** (c), **TPS$_{98}$Pt-I** (d), **TPS$_{118}$Pt-I** (e), and **TPS$_{158}$Pt-I** (f) in chloroform with the increasing concentration (3.12×10^{-6}, 6.25×10^{-6}, 1.25×10^{-5}, 2.5×10^{-5}, 5.0×10^{-5}, 1.0×10^{-4}, and 2×10^{-4} mol/L).

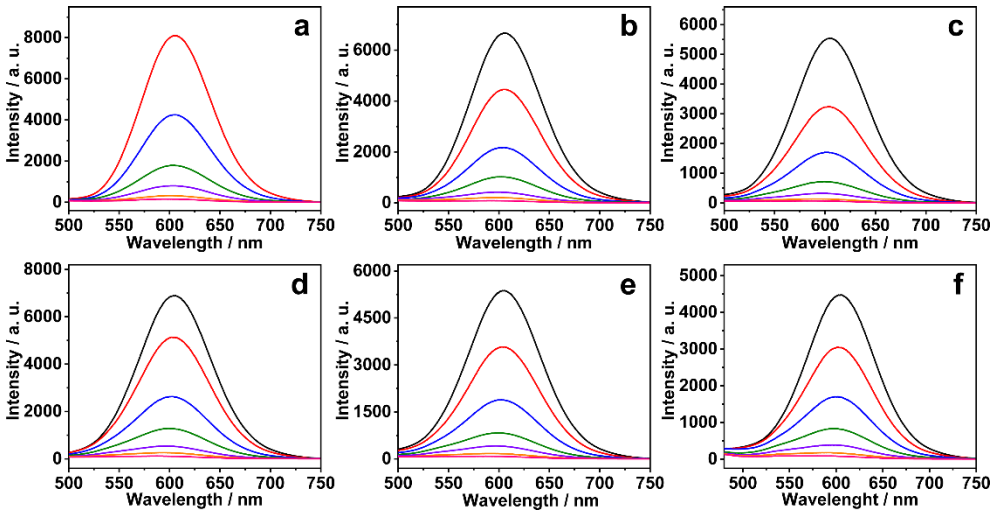

Fig. S22 Luminescence spectra of **TPS$_{26}$Pt-II** (a), **TPS$_{40}$Pt-II** (b), **TPS$_{60}$Pt-II** (c), **TPS$_{78}$Pt-II** (d), **TPS$_{98}$Pt-II** (e), and **TPS$_{158}$Pt-II** (f) in chloroform with the increasing concentration (3.12×10^{-6}, 6.25×10^{-6}, 1.25×10^{-5}, 2.5×10^{-5}, 5.0×10^{-5}, 1.0×10^{-4}, and 2×10^{-4} mol/L).

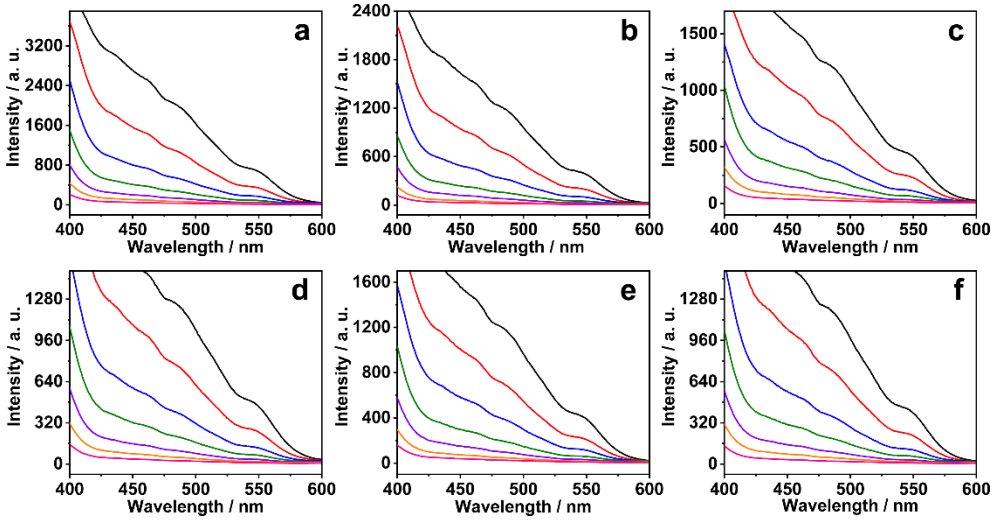

Fig. S23 Excitation spectra of **TPS$_{26}$Pt-I** (a), **TPS$_{40}$Pt-I** (b), **TPS$_{60}$Pt-I** (c), **TPS$_{98}$Pt-I** (d), **TPS$_{118}$Pt-I** (e), and **TPS$_{158}$Pt-I** (f) in chloroform with the increasing concentration (3.12×10^{-6}, 6.25×10^{-6}, 1.25×10^{-5}, 2.5×10^{-5}, 5.0×10^{-5}, 1.0×10^{-4}, and 2×10^{-4} mol/L).

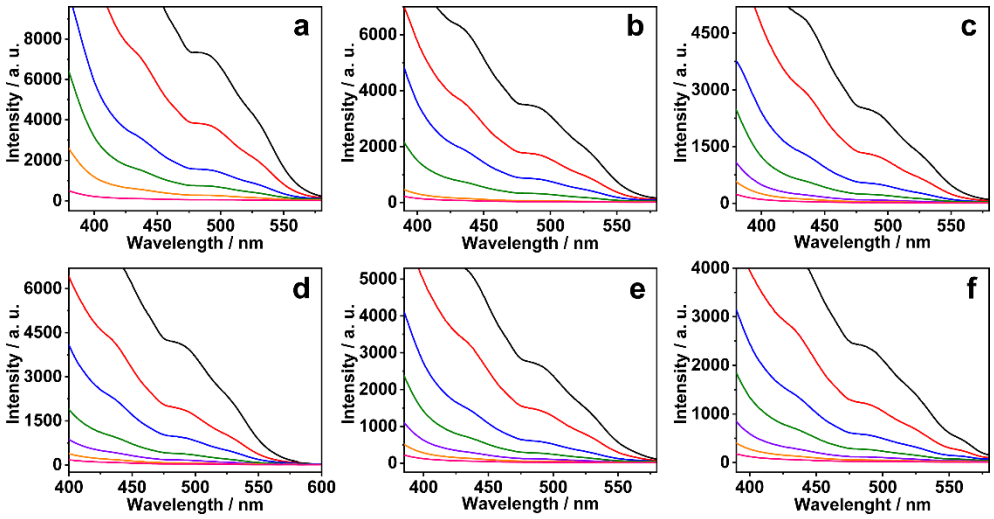

Fig. S24 Excitation spectra of **TPS$_{26}$Pt-II** (a), **TPS$_{40}$Pt-II** (b), **TPS$_{60}$Pt-II** (c), **TPS$_{78}$Pt-II** (d), **TPS$_{98}$Pt-II** (e), and **TPS$_{158}$Pt-II** (f) in chloroform with the increasing concentration (3.12×10^{-6}, 6.25×10^{-6}, 1.25×10^{-5}, 2.5×10^{-5}, 5.0×10^{-5}, 1.0×10^{-4}, and 2×10^{-4} mol/L).

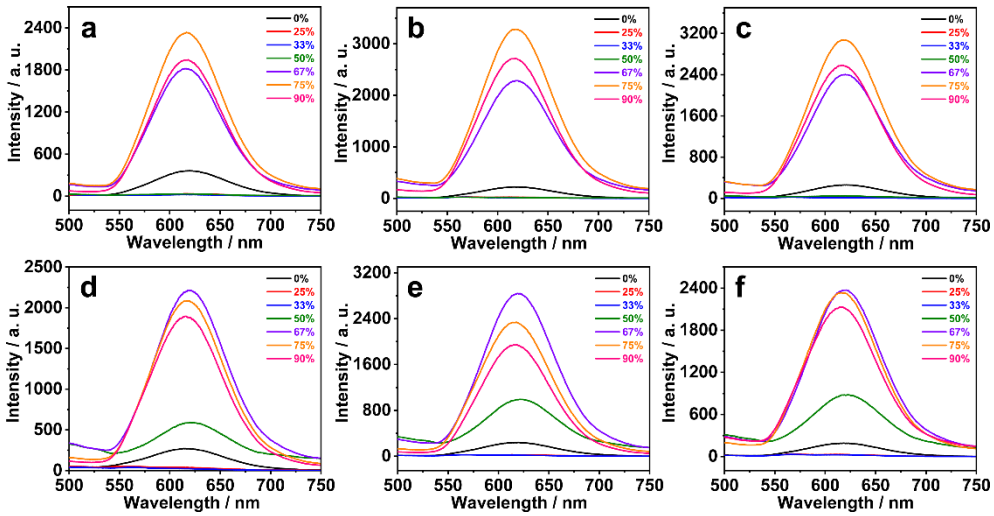

Fig. S25 Luminescence spectra of **TPS$_{26}$Pt-I** (a), **TPS$_{40}$Pt-I** (b), **TPS$_{60}$Pt-I** (c), **TPS$_{98}$Pt-I** (d), **TPS$_{118}$Pt-I** (e), and **TPS$_{158}$Pt-I** (f) in the chloroform/methanol mixture solvents. The final concentrations were 5.0×10^{-5} mol/L.

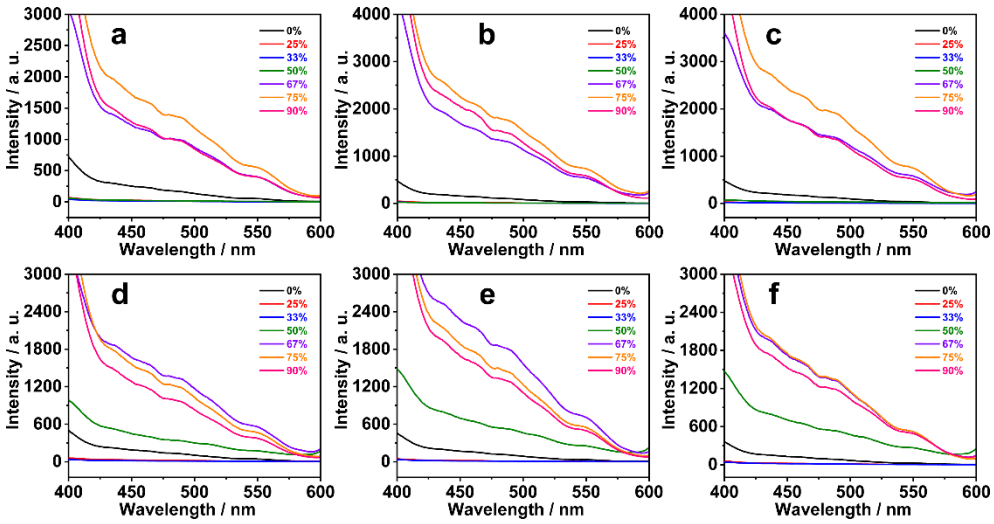

Fig. S26 Excitation spectra of **TPS$_{26}$Pt-I** (a), **TPS$_{40}$Pt-I** (b), **TPS$_{60}$Pt-I** (c), **TPS$_{98}$Pt-I** (d), **TPS$_{118}$Pt-I** (e), and **TPS$_{158}$Pt-I** (f) in the chloroform/methanol mixture solvents. The final concentrations were 5.0×10^{-5} mol/L.

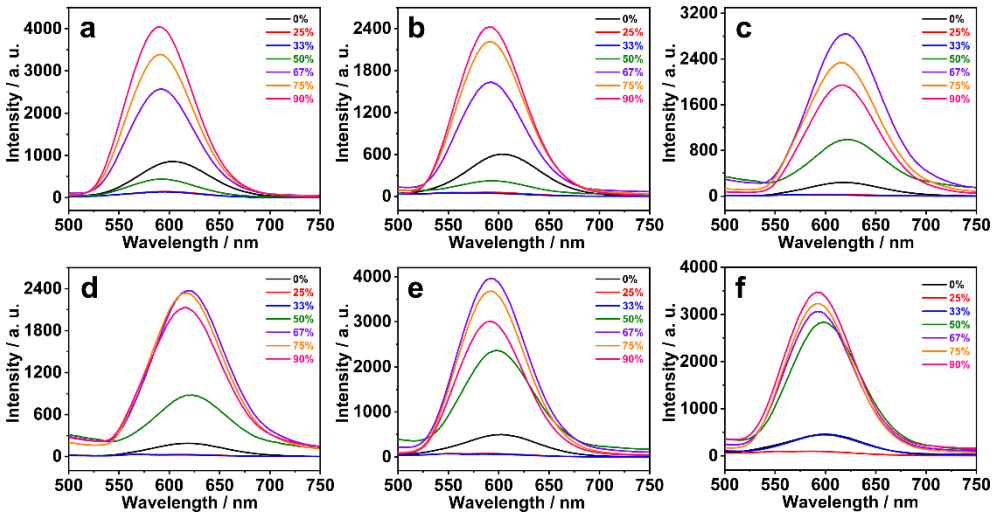

Fig. S27 Luminescence spectra of **TPS$_{26}$Pt-II** (a), **TPS$_{40}$Pt-II** (b), **TPS$_{60}$Pt-II** (c), **TPS$_{78}$Pt-II** (d), **TPS$_{98}$Pt-II** (e), and **TPS$_{158}$Pt-II** (f) in the chloroform/methanol mixture solvents. The final concentrations were 5.0×10^{-5} mol/L.

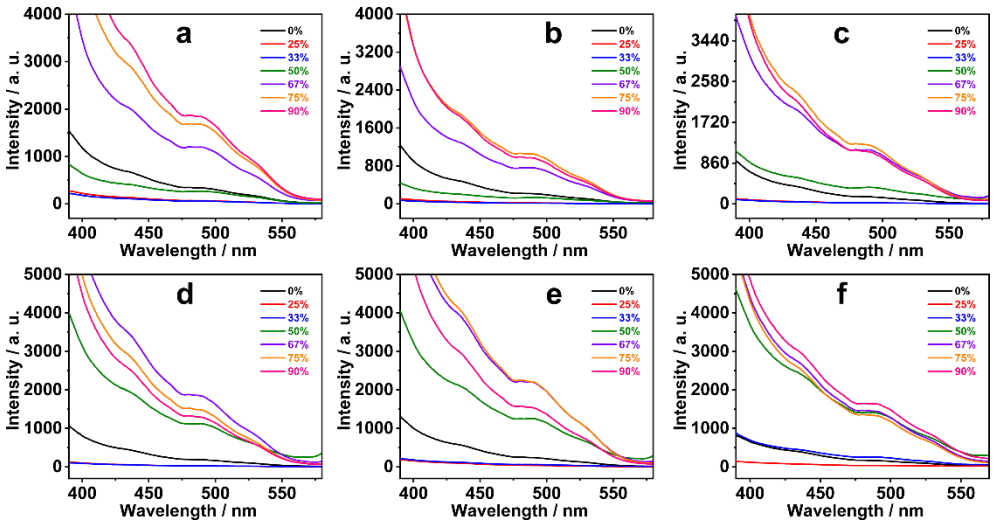

Fig. S28 Excitation spectra of **TPS$_{26}$Pt-II** (a), **TPS$_{40}$Pt-II** (b), **TPS$_{60}$Pt-II** (c), **TPS$_{78}$Pt-II** (d), **TPS$_{98}$Pt-II** (e), and **TPS$_{158}$Pt-II** (f) in the chloroform/methanol mixture solvents. The final concentrations were 5.0×10^{-5} mol/L.

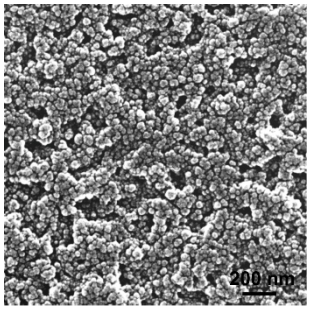

Fig. S29 SEM image of **TPS$_{118}$Pt-I** obtained in the chloroform/methanol mixture solvent with a methanol volume ratio of 90%.

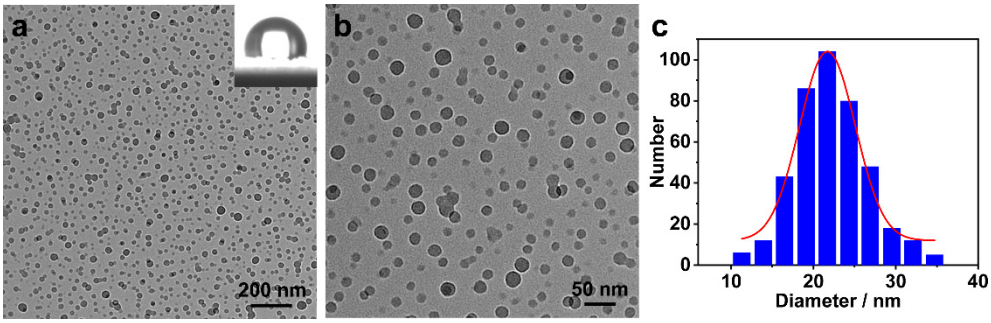

Fig. S30 TEM image (a and b) of **TPS$_{118}$Pt-I** obtained in the chloroform/methanol mixture solvent with a methanol volume ratio of 75%. (c) The flowerlike micelles had a diameter of 21.7 ± 3.4 nm.

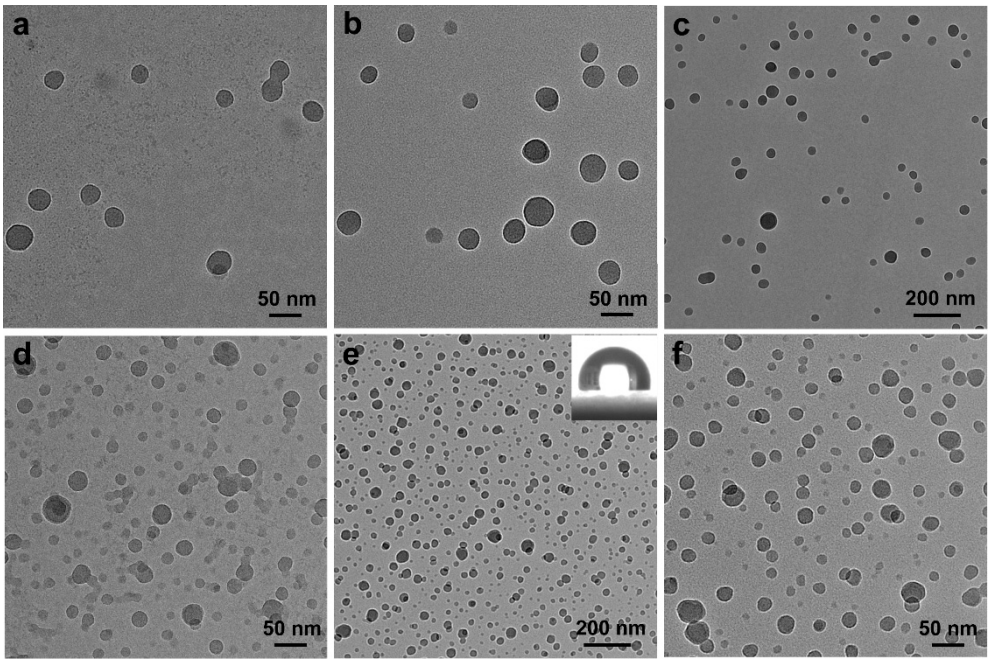

Fig. S31 TEM images of **TPS_{60}Pt-I** obtained in the chloroform/methanol mixture solvent with methanol compositions of 50 vol % (a and b), 75 vol % (c and d), and 90 vol % (e and f). The inset (e) gave a water contact angle of 108°.

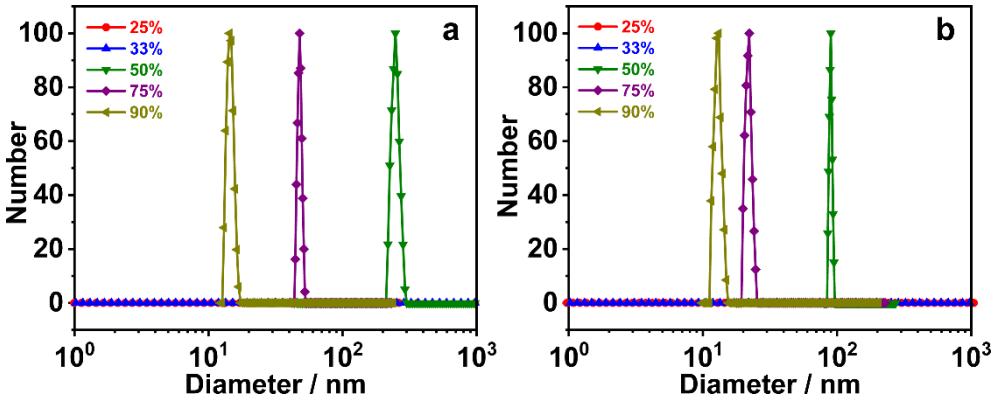

Fig. S32 DLS plots of **TPS_{78}Pt-I** (a) and **TPS_{118}Pt-II** (b) dispersed in the chloroform/methanol mixture solvents with methanol contents of 25, 33, 50, 75, and 90 vol %.

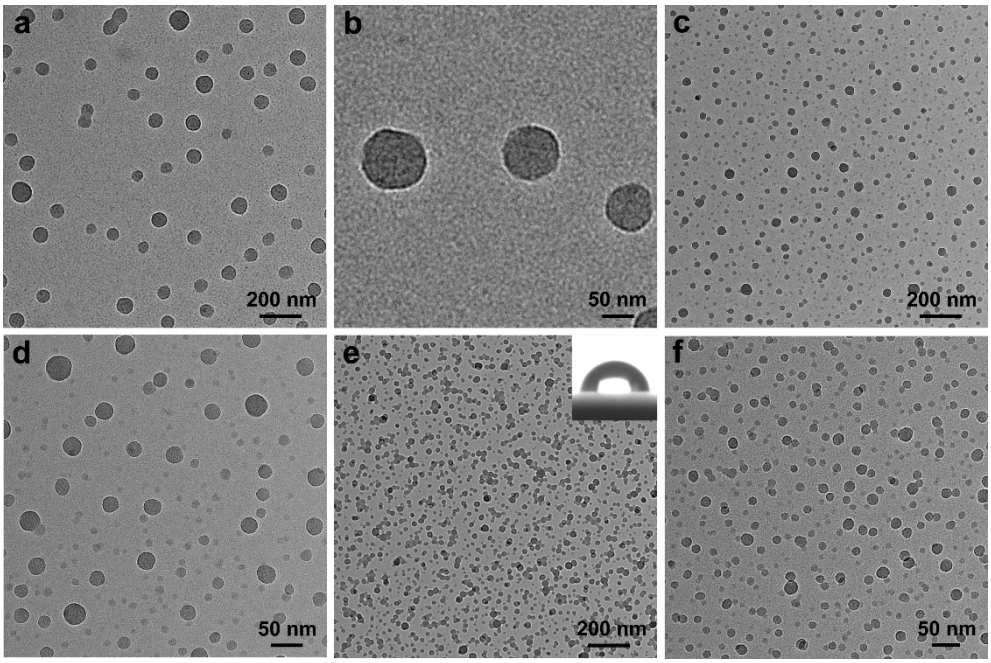

Fig. S33 TEM images of **TPS$_{78}$Pt-I** obtained in the chloroform/methanol mixture solvent with methanol compositions of 50 vol % (a and b), 75 vol % (c and d), and 90 vol % (e and f). The inset (e) gave a water contact angle of 108°.

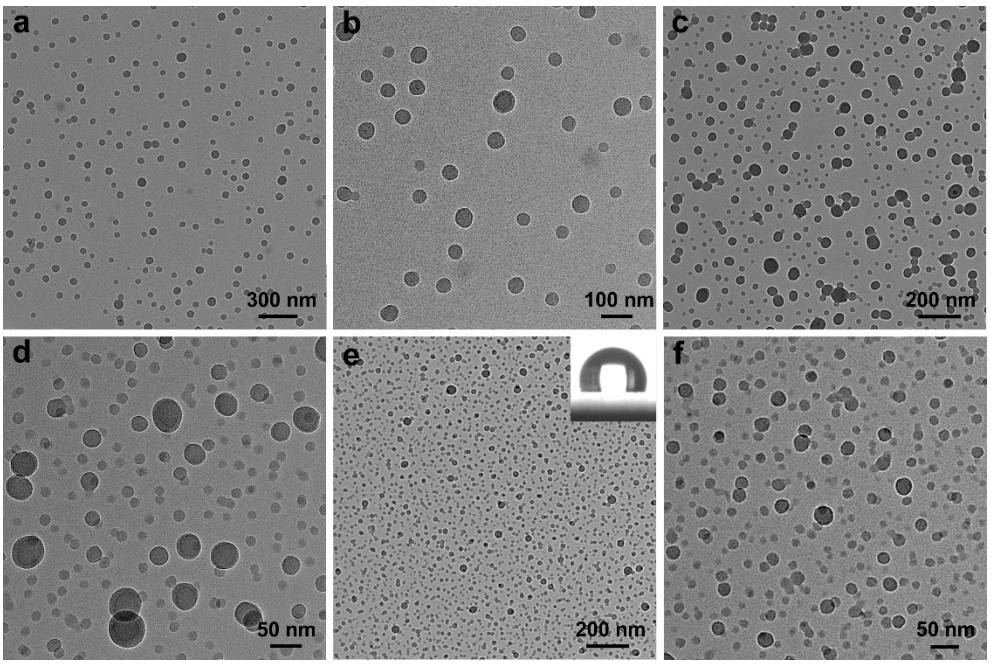

Fig. S34 TEM images of **TPS$_{98}$Pt-I** obtained in the chloroform/methanol mixture solvent with methanol compositions of 50 vol % (a and b), 75 vol % (c and d), and 90 vol % (e and f). The inset (e) gave a water contact angle of 114°.

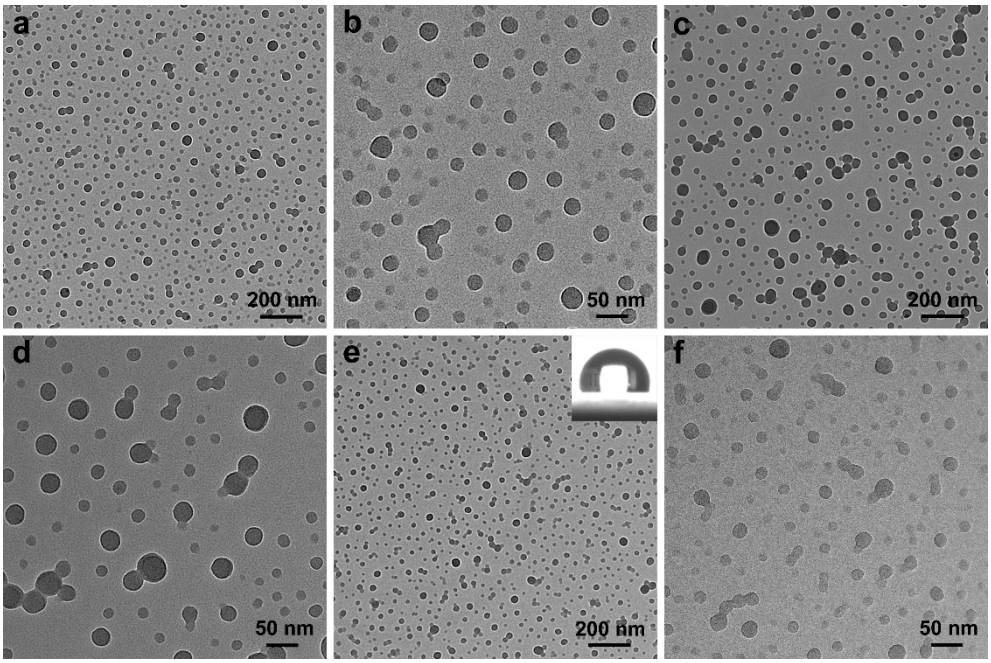

Fig. S35 TEM images of **TPS_{158}Pt-I** obtained in the chloroform/methanol mixture solvent with methanol compositions of 50 vol % (a and b), 75 vol % (c and d), and 90 vol % (e and f). The inset (e) gave a water contact angle of 115°.

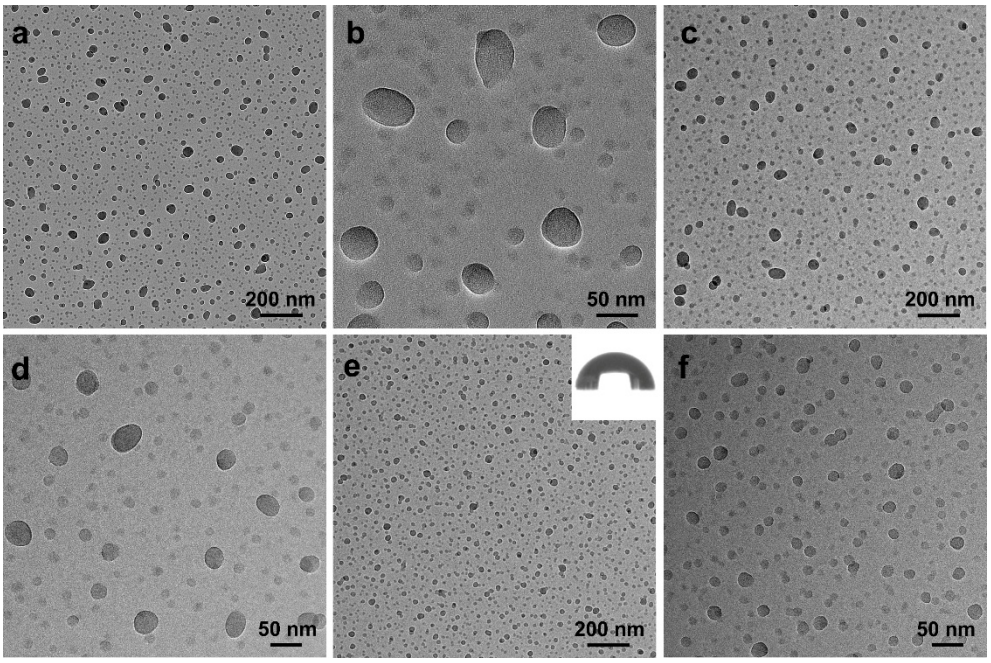

Fig. S36 TEM images of **TPS_{60}Pt-II** obtained in the chloroform/methanol mixture solvent with methanol compositions of 50 vol % (a and b), 75 vol % (c and d), and 90 vol % (e and f). The inset (e) gave a water contact angle of 97°.

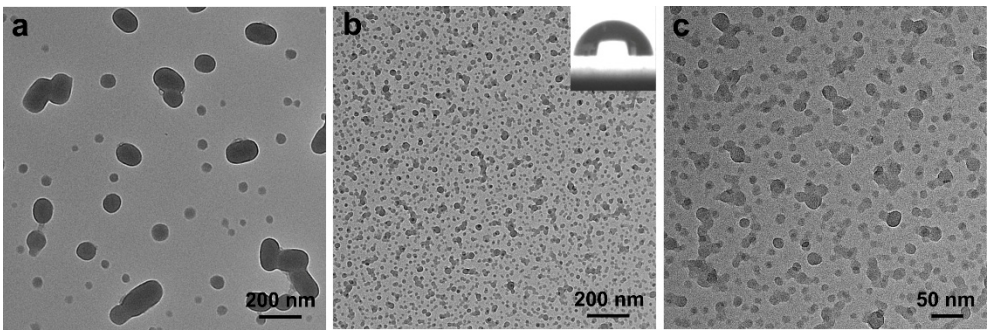

Fig. S37 TEM images of **TPS$_{78}$Pt-II** obtained in the chloroform/methanol mixture solvent with methanol compositions of 50 vol % (a) and 90 vol % (e and f). The inset (b) gave a water contact angle of 97°.

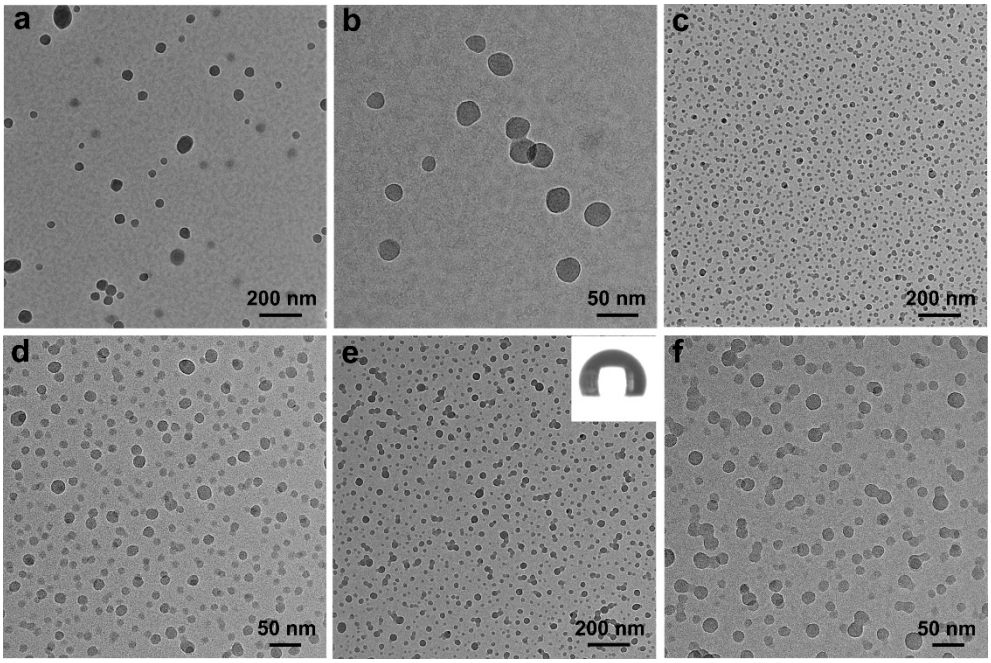

Fig. S38 TEM images of **TPS$_{98}$Pt-II** obtained in the chloroform/methanol mixture solvent with methanol compositions of 50 vol % (a and b), 75 vol % (c and d), and 90 vol % (e and f). The inset (e) gave a water contact angle of 122°.

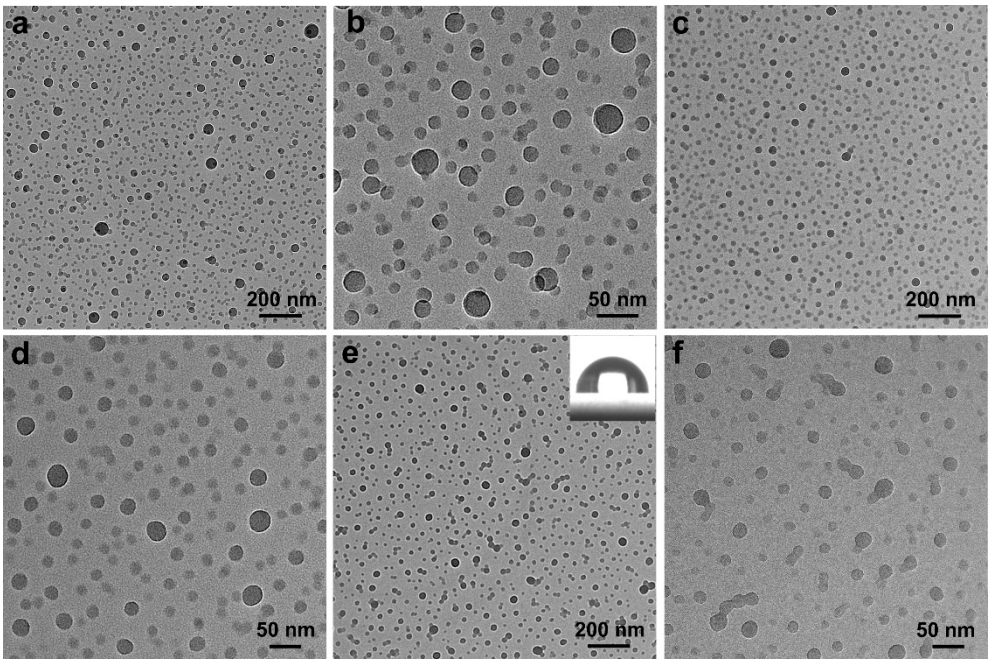

Fig. S39 TEM images of **TPS_{118}Pt-II** obtained in the chloroform/methanol mixture solvent with methanol compositions of 50 vol % (a and b), 75 vol % (c and d), and 90 vol % (e and f). The inset (e) gave a water contact angle of 120°.

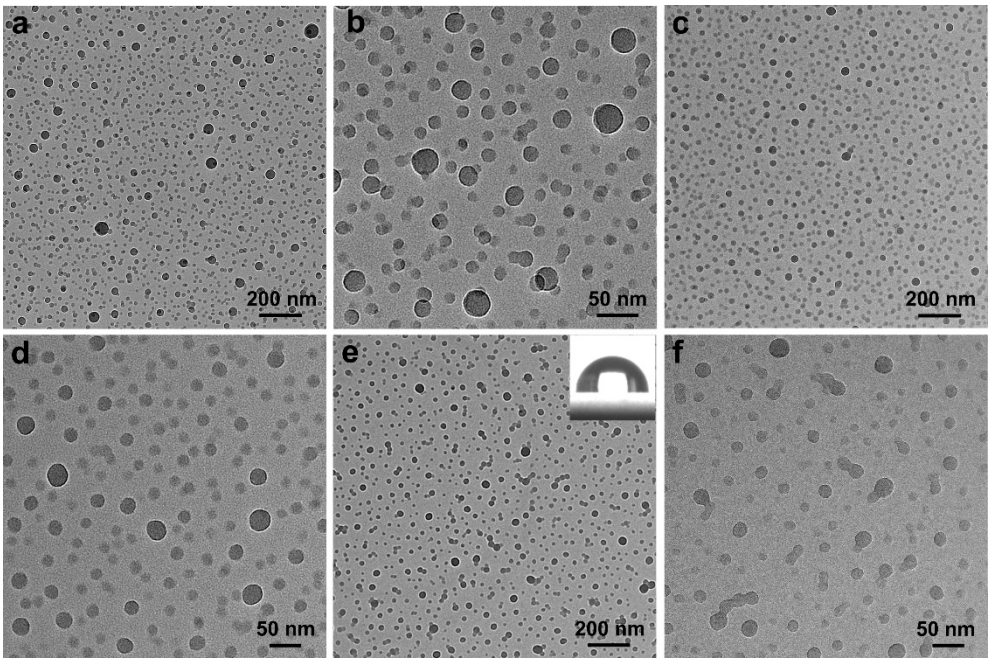

Fig. S40 TEM images of **TPS_{158}Pt-II** obtained in the chloroform/methanol mixture solvent with methanol compositions of 50 vol % (a and b), 75 vol % (c and d), and 90 vol % (e and f). The inset (e) gave a water contact angle of 118°.

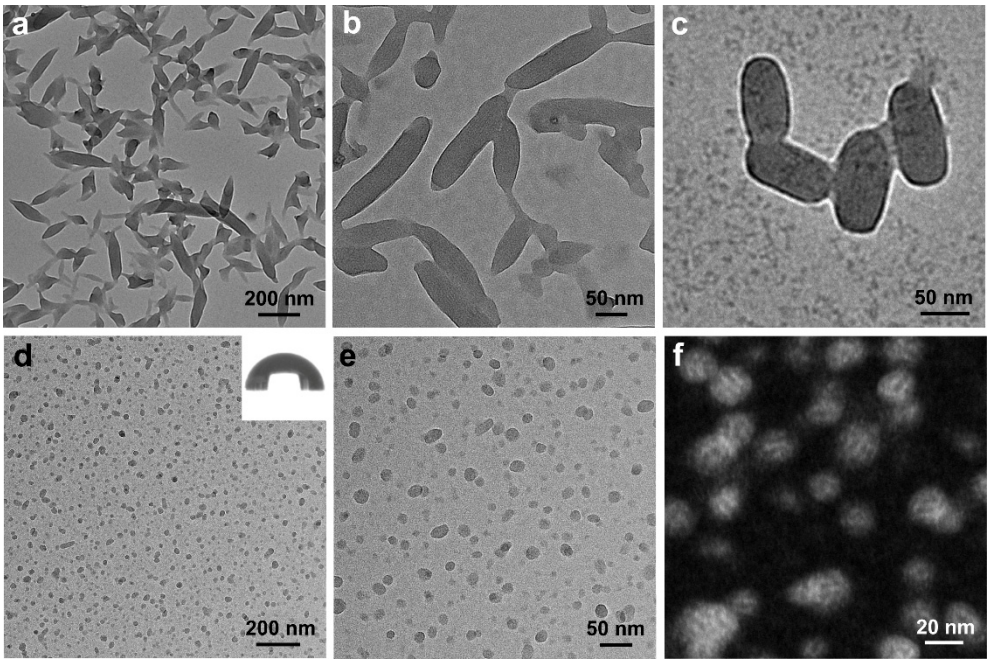

Fig. S41 TEM images of **TPS_{40}Pt-II** obtained in the chloroform/methanol mixture solvent with methanol compositions of 50 vol % (a and b), 75 vol % (c), and 90 vol % (d, e, and f). The inset (d) gave a water contact angle of 95°.

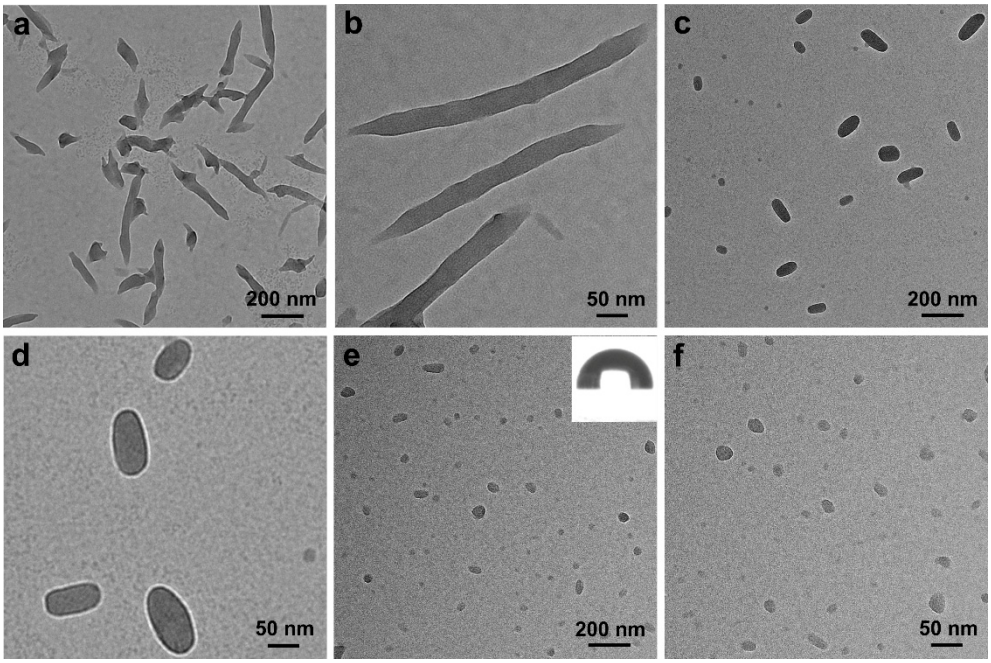

Fig. S42 TEM images of **TPS_{26}Pt-II** obtained in the chloroform/methanol mixture solvent with methanol compositions of 50 vol % (a and b), 75 vol % (c and d), and 90 vol % (e and f). The inset (e) gave a water contact angle of 98°.

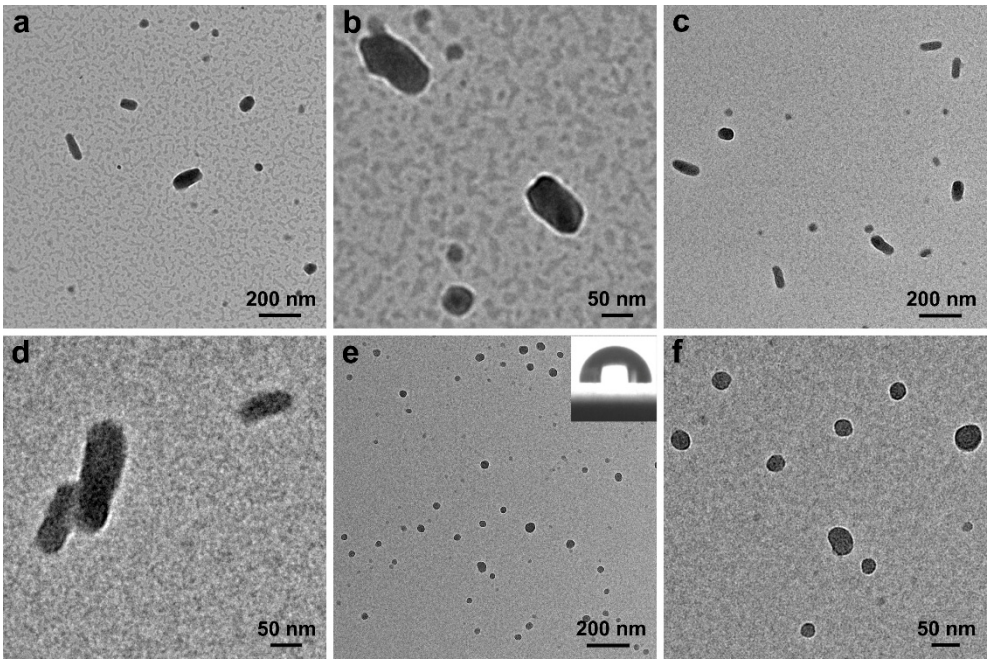

Fig. S43 TEM images of **TPS_{26}Pt-I** obtained in the chloroform/methanol mixture solvent with methanol compositions of 50 vol % (a and b), 75 vol % (c and d), and 90 vol % (e and f). The inset (e) gave a water contact angle of 98°.

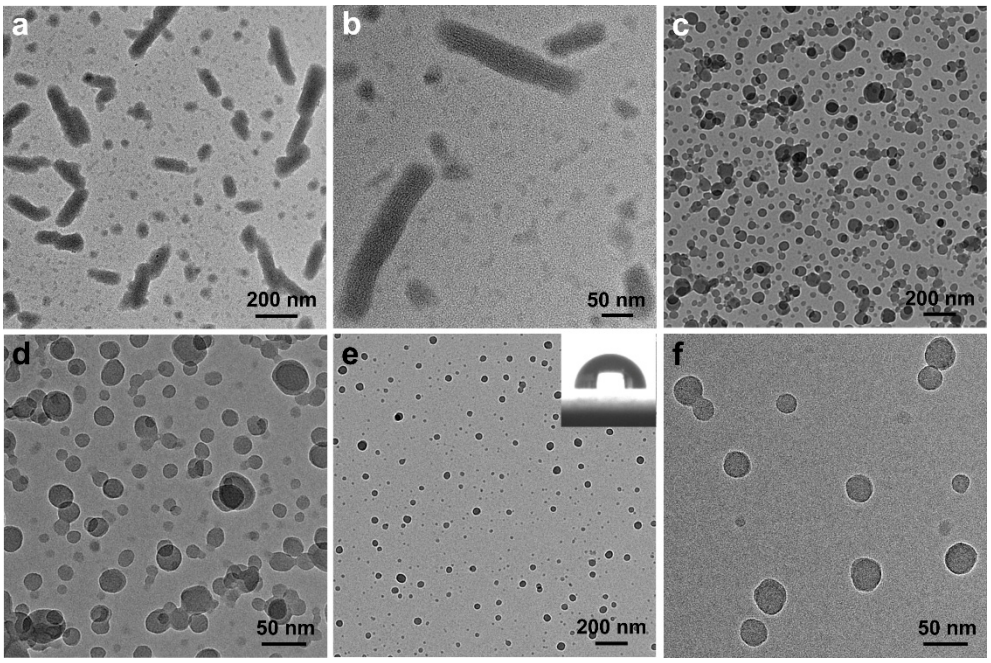

Fig. S44 TEM images of **TPS_{40}Pt-I** obtained in the chloroform/methanol mixture solvent with methanol compositions of 50 vol % (a and b), 75 vol % (c and d), and 90 vol % (e and f). The inset (e) gave a water contact angle of 97°.

REFERENCES

(S1) C. Rajnák, J. Titiš, O. Fuhr, M. Ruben and R. Boča, *Polyhedron*, 2017, **123**, 122.

(S2) F. Qu, B. Yang, Q. He and W. Bu, *Polym. Chem.,* 2017, **8**, 4716.

(S3) W. Meng, X. Qiu, R. Wang, Q. He and W. Bu, *J. Mater. Chem. C*, 2020, **8**, 15616.

(S4) J. Van Houten and R. J. Watts, *J. Am. Chem. Soc.*, 1976, **98**, 4853.

(S5) G. A. Crosby and J. N. Demas, *J. Phys. Chem.*, 1971, **75**, 991.